Ibn Al-Haitham Journal for Pure and Applied Sciences
Journal homepage: jih.uobaghdad.edu.iq
PISSN: 1609-4042, EISSN: 2521-3407
IHJPAS. 2026; 39(2)

Effect of Graphene Oxide Concentration on the Antibacterial Activity of GO–ZnO Hybrid Nanocomposites

Ruaa F. Fadhil[1], Hind F. Oleiwi[2]*, and Sanaa T. Sarhan[3]
[1,3]Department of Chemistry, College of Science for Women, University of Baghdad, Baghdad, Iraq
[2]Department of Physics, College of Science for Women, University of Baghdad, Baghdad, Iraq
*Corresponding Author

Received: 20/August /2025
Accepted:14/December/2025
Published: 20 /April/2026
doi.org/10.30526/39.2.4285

Abstract

Graphene oxide (GO) with zinc oxide nanoparticles (ZnO NPs) was synthesized using sol-gel and spin-coating procedures. This study aims to assess the antibacterial properties of ZnO-GO nanocomposites produced by spin coating with varying GO concentrations. So, different concentrations of GO NPs (10%, 30%, and 50%) were added to ZnO to assess the antibacterial activity. Structural and morphological properties of ZnO-GO were characterized using X-ray diffraction, field-emission scanning electron microscopy (FE-SEM), energy dispersive X-ray spectroscopy, and atomic force microscopy. The crystalline size of the pure ZnO NPs decreases with the increase of GO concentration, and the average crystalline size is 32.875 nm. The FESEM images showed that all samples contained mostly spherical-shaped particles with a high tendency to agglomerate. Also, the antimicrobial activity of the synthesized NPs (ZnO-GO) was investigated against the Gram-positive bacterium *Staphylococcus aureus*, the Gram-negative bacterium *Escherichia coli*, and the fungus *Candida albicans*. The antibacterial properties of three compounds were highly efficient. Additionally, it was demonstrated that ZnO-GO has higher antibacterial activity than pure ZnO NPs.

Keywords: Bacterial effectiveness, Graphene oxide, Nanocomposite, Spin-coating technique, Zinc oxide.

1. Introduction

Nanotechnology is a multidisciplinary approach to the biochemical applications of antioxidants and antibacterials, which are currently being studied for their potential to treat cancer and degenerative diseases[1]. Employs interdisciplinary strategies to focus on biochemical applications, and now antibacterial and antioxidant nanoparticles (NPs) are believed to protect against cancer and degenerative diseases[2,3]. All biological systems need antioxidants to function correctly, and these result from the interaction of bimolecular with free radicals, molecular oxygen, and bimolecular degradation[4]. Thus, to stop oxidative stress and its harmful effects, natural antioxidants must be produced[5]. These free radicals are neutralized by certain NPs, thereby preventing oxidative damage to the human body. In this context, green NPs with antioxidant properties can be used[6]. ZnO NPs are one type of NP that has been studied for use in industry and science in recent decades[7]. Furthermore, ZnO NPs reduce antibacterial activity by acting as a mitochondrial respiratory regulator, leading to an overabundance of free radicals. According to earlier research, ZnO-NPs are not harmful to human cells. They are used as antibacterial agents, harming microorganisms and adapting to human cells[8]. The accumulation of ZnO NPs results from van der Waals forces and surface effects, which erode their distinctive chemical characteristics and eliminate their antibacterial activity[9]. Consequently, to minimize aggregation, the number of ZnO particles ought to include sites with an inorganic or organic, stable polymer reaction. Many researchers are therefore interested in developing unique and

potent cytotoxic, antibacterial, or anticancer compounds[10]. The antibacterial properties of Zn-NPs can be significantly enhanced by combining their surface with graphene[11]. Attractive characteristics of graphene oxide (GO) include its high surface-to-volume ratio, excellent optical brightness, and electronic transport capabilities[12]. It can serve as a foundation for the development and stabilization of NPs and prevent their accumulation; this may ultimately lead to a more stable arrangement with potent antibacterial and anticancer activity[13,14]. The distribution and stabilization of GO with ZnO particles enhance antibacterial performance and improve bacterial interactions. It increases surface area, inhibits agglomeration, and encourages the production of reactive oxygen species (ROS)[15,16]. GO/ZnO concentration is critical—low concentrations are often optimal. A layer of ZnO/GO can significantly improve properties and reduce bacterial colony counts without causing harmful effects[17]. In addition, antibacterial systems have several interdependent mechanisms. ZnO causes bacterial membrane disruption and releases Zn^{2+} ions. Charge separation, electron transfer, and ROS production are all improved by the addition of GO, thereby strengthening antibacterial synergy[18,19]. When graphene is exposed to bacterial cells, it interacts chemically and physically, thereby exerting antimicrobial activity. Graphene's surface and edge functional groups provide antibacterial properties. Because graphene is oxidative and releases ROS, its sharp edges damage cell membranes and promote oxidative stress[20]. This study aims to assess the antibacterial properties of ZnO/GO nanocomposites produced by spin coating with varying GO concentrations.

2. Materials and Methods

2.1. Synthesis methods

ZnO NPs were obtained by first synthesizing the solution via the sol-gel process, then depositing it via spin coating, and finally annealing. The sol-gel method, which uses a sol-gel solution, is regarded as an easy and efficient oxidation technique[21,22]. To prepare a stable sol-gel for the deposition procedure, 0.2 M Zn acetate dihydrate [$Zn(CH_3CO_2)_2.2H_2O$] and diethanolamine (DEA) were dissolved in ethanol, and the mixture was stirred for 1 hr until clear. Next, the solution was aged for 1 day at room temperature. The precipitate was filtered, washed, and dried with distilled water and ethanol. The dried powder was calcined at 400°C. The soda-lime glass slides (2×2×0.2 cm^3) are cleaned and washed with deionized water (DI), acetone, and 2-propanol using sonication for 20 minutes. To ensure that all surface impurities were removed, the substrate was then dried in an oven. Then, 20.0 g/L of ZnO NPs were dissolved in ethanol with varying percentages of GO 99.8% powder (10%, 30%, and 50%). The precursor solution was then evenly distributed over the glass slides after ZnO and ZnO-GO were deposited via spin coating at 3000 rpm for 30 minutes. The samples were annealed in a furnace at 300°C for 1 hr.

2.2. Biological activity

The inhibitory efficacy was assessed against all harmful pathogens; Mueller-Hinton agar was utilized[23]. In this study, 9-cm-diameter Petri dishes were employed. A central well with a diameter of 8 mm was prepared in each dish, into which the test materials (ZnO-GO) were introduced at varying concentrations: Pure ZnO, $_{90}ZnO/_{10}GO$, $_{70}ZnO/_{30}GO$, and $_{50}ZnO/_{50}GO$. The volume of each material introduced was 100 µL, and the dish height was 4 mm. Bacterial suspensions at a concentration of 1.5×10^8 cells/mL were applied around the well. The plates were then incubated for 24 hours to allow bacterial growth and to facilitate diffusion of the nanomaterials into the well. After incubation, the well diameter was measured. An increase in diameter beyond 8 mm was interpreted as indicating antibacterial activity, whereas a diameter of 8 mm suggested that the material had no inhibitory effect on bacterial growth. All experiments were performed in triplicate, and the mean inhibition diameter was calculated to ensure the reliability of the results.

2.3. Characterization

Chemical techniques have been used, and the field emission scanning electron microscope (FESEM) was coupled to the energy-dispersive X-ray (EDX) device to produce topographic

images and top views of the ZnO and ZnO/GO with different GO concentrations (TESCAN MIRA3 FRENCH). The structural properties of various materials were examined using the X-ray diffraction (XRD 6000) technique (SHIMADZU Japan) in a mode 2 system diffractometer with a copper target (Cu Kα, 1.5406 Å).

3. Results

3.1. The XRD analysis

The structural properties of ZnO NPs were analyzed via XRD and are presented in **Figure 1**. The Debye-Scherrer equation was used to determine the NPs crystalline size (D), as shown in the following **Equation 1:**

$$D = \frac{K\lambda}{\beta \cos\theta} \quad \textbf{(1)}$$

Where K represents the Scherrer constant (0.98), λ denotes the wavelength (1.54 A^{o}), β denotes the full width at half maximum (FWHM), and θ is the Bragg angle shown in **Table 1**.

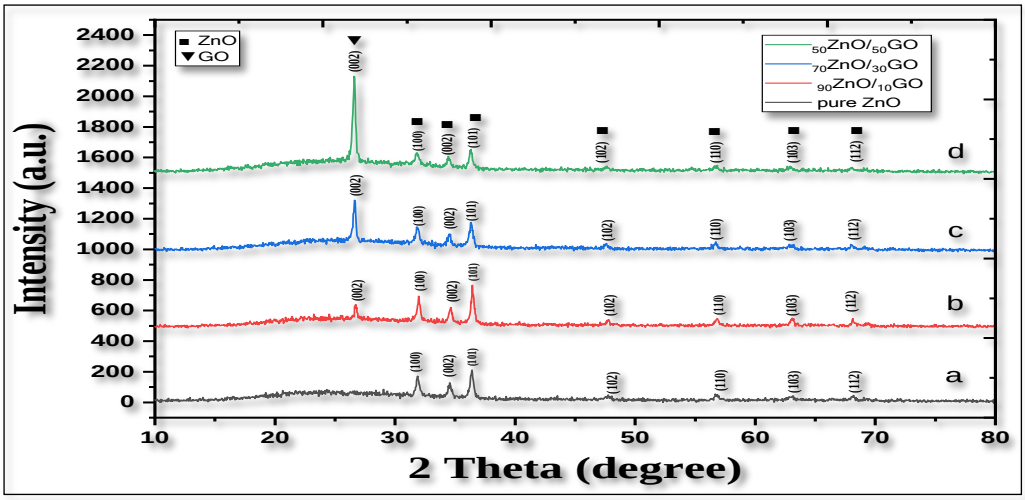

Figure 1. The XRD pattern for (a) pure ZnO, (b) $_{90}$ZnO/$_{10}$GO, (c) $_{70}$ZnO/$_{30}$GO, and (d) $_{50}$ZnO/$_{50}$GO

Table 1. Crystal size for pure ZnO NPs and ZnO/GO nanocomposite

Samples	2θ (deg.)	FWHM (deg.)	D (nm)
Pure ZnO	44.257	0.264	32.4
$_{90}$ZnO/$_{10}$GO	41.367	0.353	24.1
$_{70}$ZnO/$_{30}$GO	43.060	0.215	39.8
$_{50}$ZnO/$_{50}$GO	43.452	0.243	35.2

3.2. The FESEM results

An advanced method, field-emission scanning electron microscopy (FE-SEM), was used to capture images of the materials' microstructure. **Figure 2** displays bare top-view FESEM images with various scales for ZnO and ZnO/GO nanocomposites with different concentrations (pure ZnO, $_{90}$ZnO/10GO, $_{70}$ZnO/$_{30}$GO, and $_{50}$ZnO/$_{50}$GO). It has been indicated that all images of ZnO and ZnO/GO NPs show average particle sizes below 100 nm.

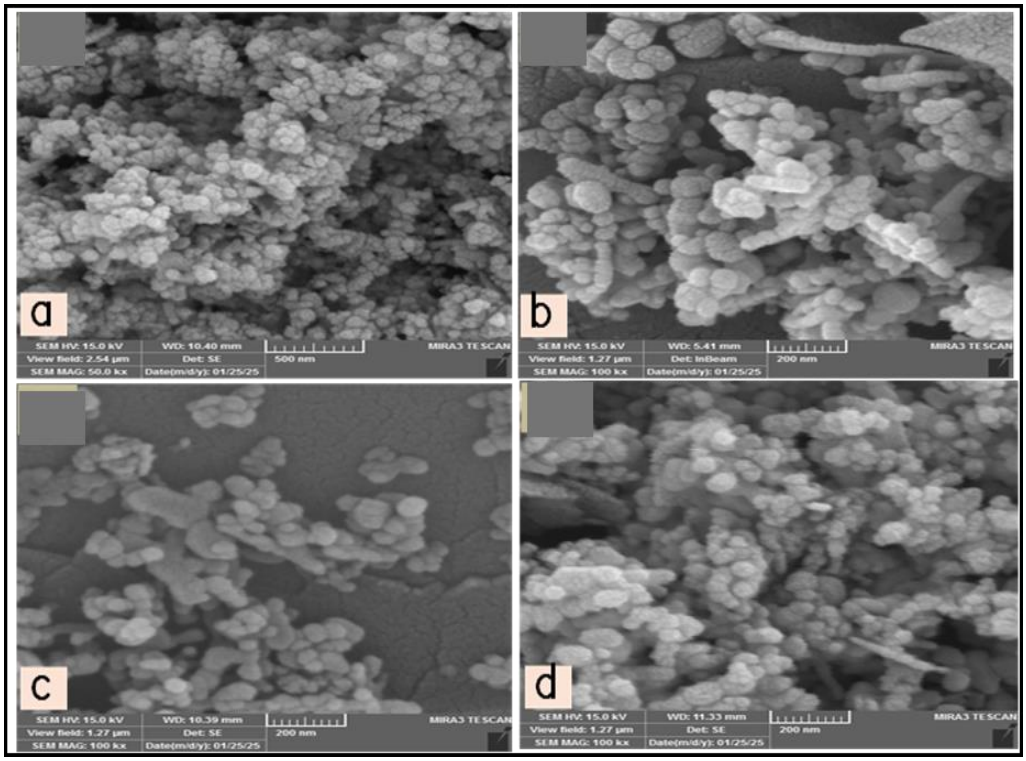

Figure 2. Top-view FESEM images for (a) Pure ZnO (b) $_{50}$ZnO/$_{50}$GO, (c) $_{70}$ZnO/ $_{30}$GO, and (d) $_{90}$ZnO/$_{10}$GO

3.3. Energy-dispersive X-ray analysis

The EDX results in **Table 2** indicate the presence of Zn and O elements and demonstrate the formation of pure ZnO micronutrient. ZnO NPs were combined with GO NPs at different concentrations, as seen in **Figure 3**.

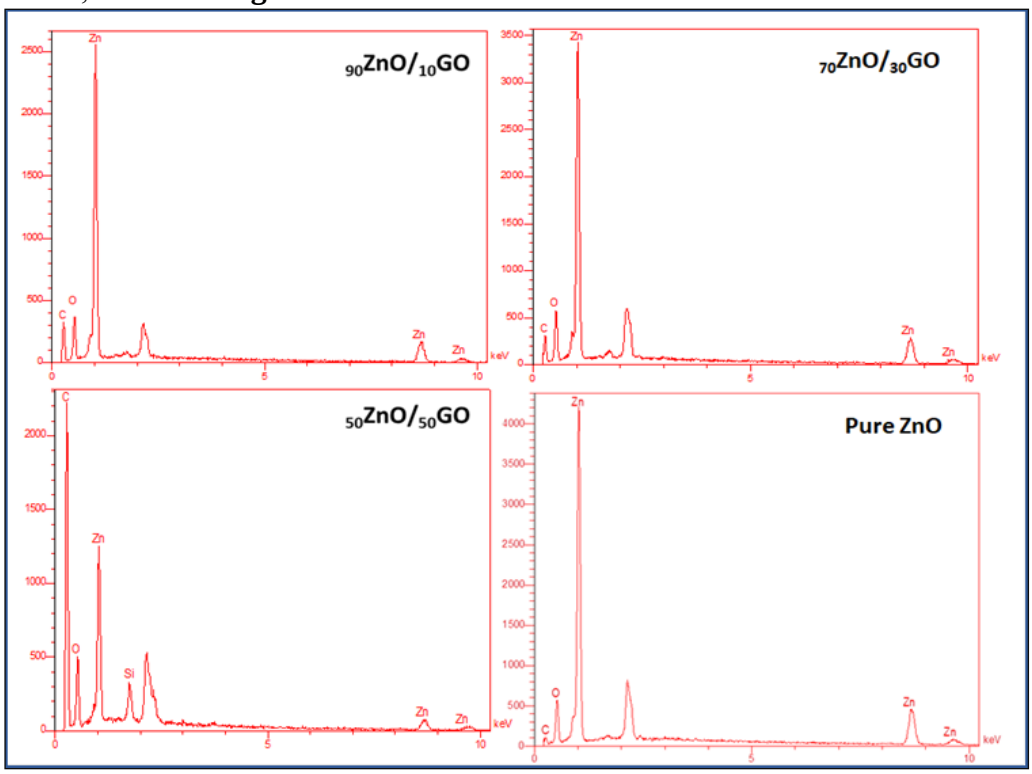

Figure 3. The EDX spectrum for pure ZnO NPs and ZnO/GO nanocomposite

Table 2. Elements Wt.% for pure ZnO NPs and ZnO/GO nanocomposite

Samples	Elements (Wt.%)			
	Zn	O	C	Si
Pure ZnO	75.24	14.64	10.12	-
$_{90}$ZnO/$_{10}$GO	47.54	18.80	33.66	-
$_{70}$ZnO/$_{30}$GO	56.27	18.73	25.00	-
$_{50}$ZnO/$_{50}$GO	11.25	20.84	65.39	2.52

3.4. Atomic force microscopy (AFM)

Nanoparticles of pure ZnO and ZnO/GO were added in different GO weight percentages ($_{90}$ZnO/$_{10}$GO, $_{70}$ZnO/$_{30}$GO, $_{50}$ZnO/$_{50}$GO) as shown in **Figures 4** and **5**.

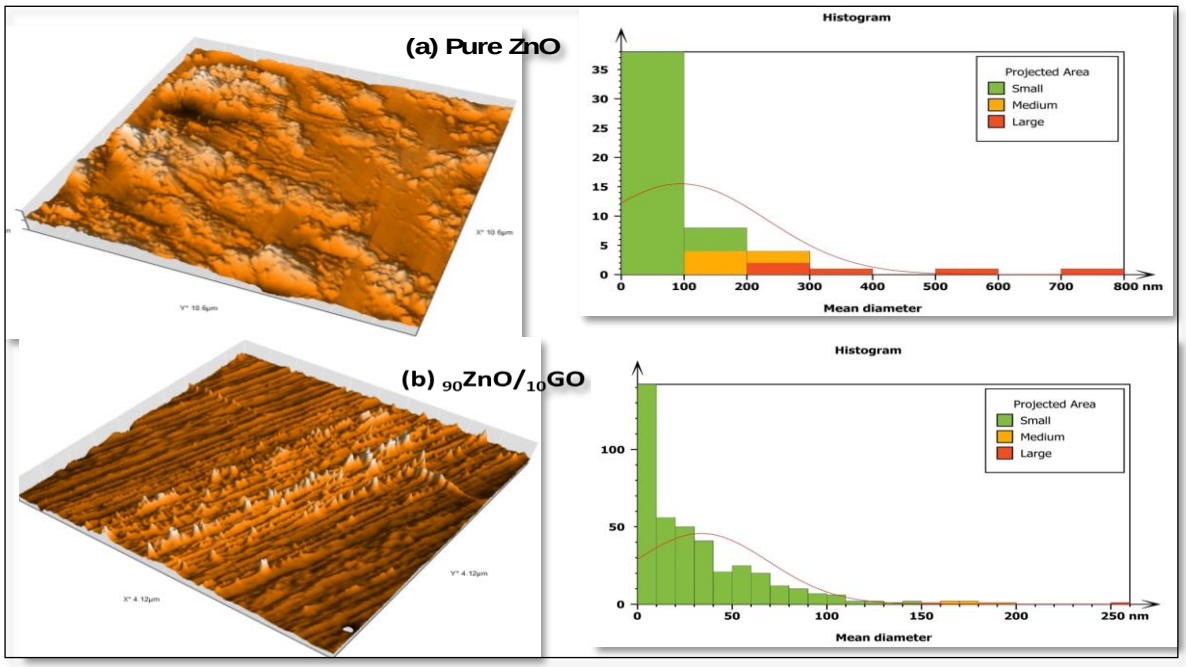

Figure 4. Topographical AFM images (2D and 3D) and particle size histograms of (a) pure ZnO (b) $_{90}$ZnO/$_{10}$GO

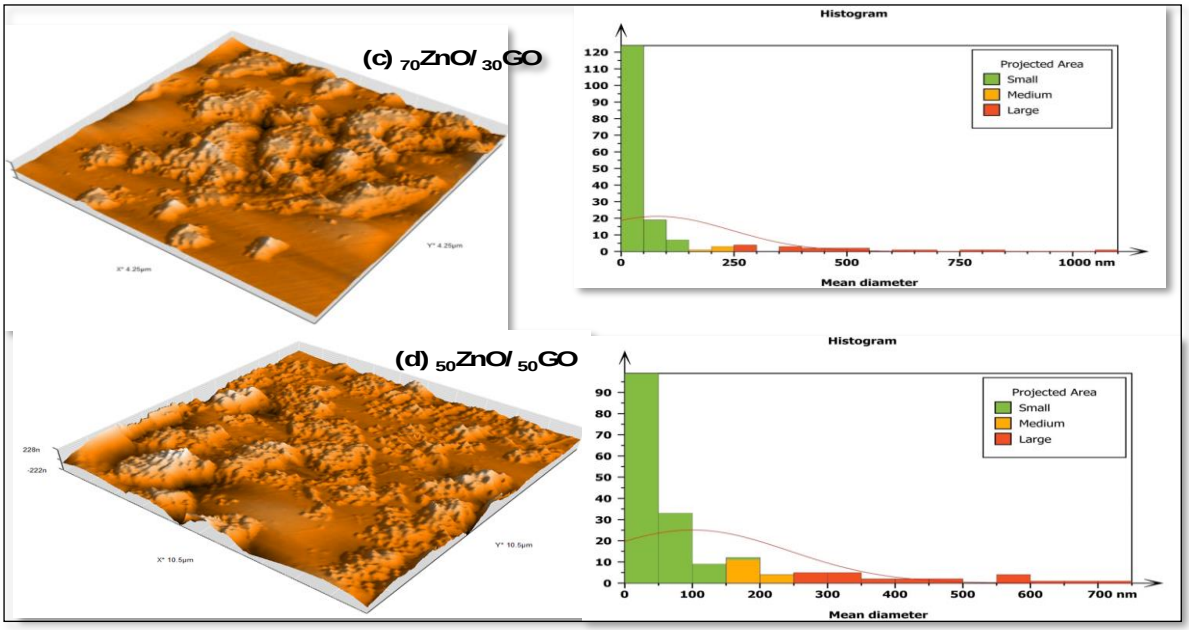

Figure 5. Topographical AFM images (2D and 3D) and particle size histograms of (c) $_{70}$ZnO/$_{30}$GO (d) $_{50}$ZnO/$_{50}$GO

3.5. Evaluation of antibacterial activity

By forming distinct zones on Mueller-Hinton agar plates, the ZnO/GO NPs inhibited the organisms' growth, as shown in **Figure 6** and **Table 3**.

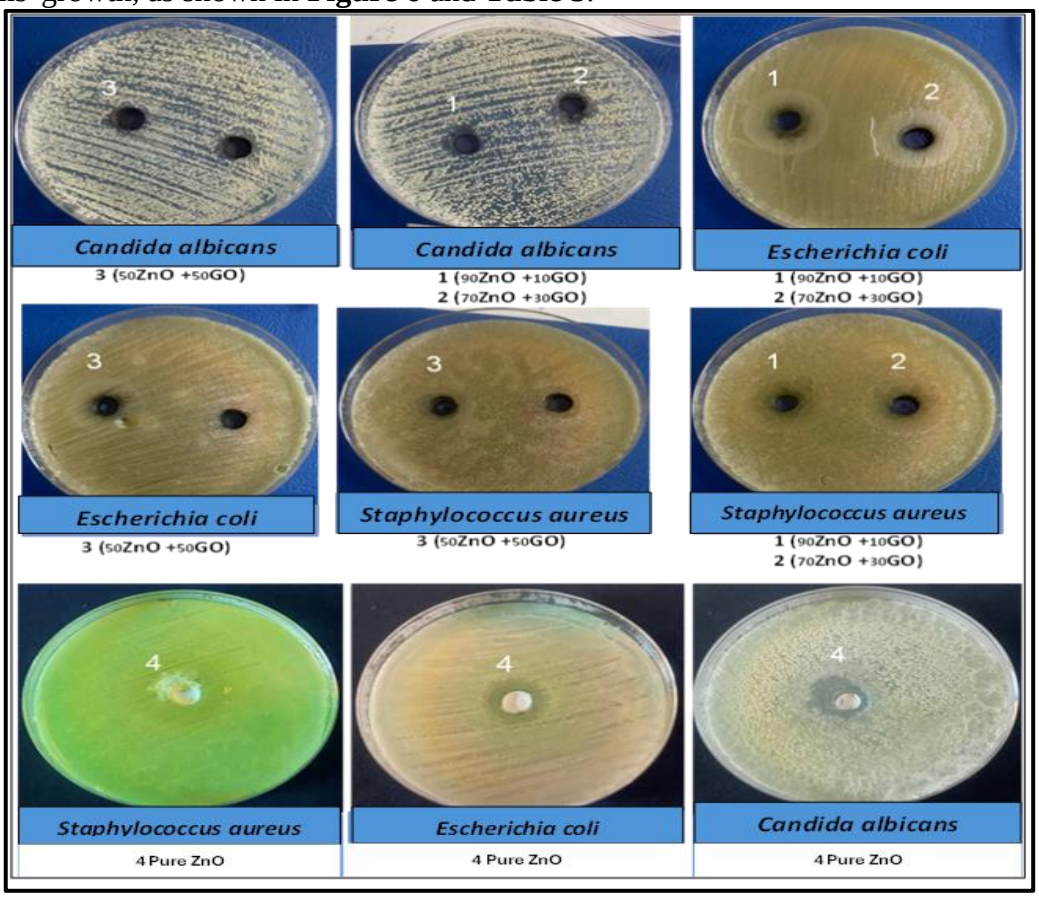

Figure 6. Effectiveness of Gram-positive bacteria, Gram-negative bacteria, and *Candida albican*

Table 3. Antibacterial activity of pure ZnO NPs and ZnO/GO nanocomposite

Samples	Diameter of inhibition zone (mm)		
	Staphylococcus. aureus	***E. coli***	***Candida***
Pure ZnO	10	20	19
$_{90}$ZnO/$_{10}$GO	27	28	13
$_{70}$ZnO/$_{30}$GO	25	26	14
$_{50}$ZnO/$_{50}$GO	15	22	14

4. Discussion

The XRD is one of several nondestructive scientific methods that provide comprehensive information about a material's physical characteristics, chemical composition, and crystallographic structure[24]. For pure ZnO, the XRD patterns obtained in this study are in agreement with the documented standard spectrum, which corresponds to the hexagonal phase (JCPDS No. 01-079-0205) and shows peaks at 2θ values of 31.85°, 34.55°, 36.35°, and 56.75°. These peaks were indexed as (100), (002), (101), and (110), respectively. No other impurity peaks were identified. The results of XRD analysis show more ZnO peaks with increasing GO concentration and fewer ZnO peaks at higher GO concentrations. The crystalline size of the pure ZnO NPs decreases for the $_{90}$ZnO/$_{10}$GO sample, then increases. When ZnO particles were intercalated into the ZnO/GO composites, they caused damage to the normal stack of GO, which is why the (002) reflection of GO appeared in the XRD pattern[24]. All samples contain almost spherical particles with a strong tendency to aggregate, as shown in the FESEM images[25]. The FESEM investigation indicates that the ZnO concentration strongly influences the shape of the final nanocomposite. These findings match those of other studies quite well[26,27].

The EDX analysis is a method that uses SEM to measure NPs. This method uses EDX, typically found in contemporary SEMs, to evaluate the NPs by activation. An atomic force microscope (AFM) can be used to analyze surface topography and determine surface height and structure. This technique enables the assessment of quantitative surface characteristics, such as roughness (Rq) and average roughness (Ra). Plot topographies can be analyzed using an AFM to assess surface elevation and structure. This technique enables quantification of surface characteristics and analysis of digital images from multiple viewpoints, including 3D modeling[28]. The nanocomposite was successfully prepared on a glass substrate by spin coating and shows AFM images and a chart of the grain density distribution of the ZnO/GO, which adheres well to the glass substrate and has a high density. The incorporation of different concentrations of pure ZnO with GO NPs changed the morphology and properties of the ZnO NPs.

The effectiveness of ligands and metal complexes against dangerous bacteria in aerobic environments was evaluated using the well diffusion method. To determine the antibacterial properties of the ZnO/GO and pure ZnO NPs, a qualitative agar diffusion test was performed. Tests were conducted for *Candida albicans*, *Staphylococcus aureus*, and *Escherichia coli*[29]. The following ratios were employed for screening: $_{50}$ZnO/$_{50}$GO, $_{70}$ZnO/$_{30}$GO, $_{90}$ZnO/$_{10}$GO, and pure ZnO. Consequently, the size of the zone of inhibition, which indicates how sensitive the organism is to the NPs, can be used to determine the concentration of the NPs and to display the inhibitory zones, measured in millimeters, created around the NPs and the positive control (the antibiotic neomycin)[30]. The GO–ZnO hybrid nanocomposites exhibit enhanced antibacterial and antifungal activity compared with either ZnO NPs or GO alone. This enhancement arises from a synergistic interplay between physicochemical and biological mechanisms that reinforce one another, leading to superior microbial inhibition, particularly against Gram-positive and Gram-negative bacteria and several fungal strains.

GO–ZnO hybrid materials exhibit higher antibacterial activity due to multi-mechanistic interactions rather than a single dominant effect; by acting as two-dimensional supports, GO enhances consistent contact with microbial membranes, increases the exposed active surface area, and inhibits ZnO NP agglomeration. The GO nanocomposite's high aspect ratio and sharp edges can physically damage cell membranes, increase permeability, and facilitate the entry of ROS and Zn^{+2} ions into microbial cells. Under light excitation, ZnO NPs produce ROS ($^{\bullet}OH$, $^{\bullet}O_2^-$, and H_2O_2). By promoting efficient charge separation and delaying electron-hole recombination, the hybrid system, when combined with GO, generates more ROS over an extended period, thereby effectively destroying cellular components. Zn^{+2} ions are controlled by GO, which maintains a constant release to extend antibacterial and antifungal activity without rapidly depleting ions.

5. Conclusion

The ZnO/GO was successfully produced using the spin-coating method at varying concentrations of GO with the ZnO precursor. The XRD patterns for ZnO/GO films demonstrate that a single phase with a hexagonal crystal structure exists. A (002) central peak can be seen in the XRD patterns, which is caused by ZnO/GO crystals that are growing along the c-axis. As the ZnO/GO NP concentration rose, the crystallite size also increased. The films' surfaces have some degree of roughness. Pure ZnO exhibited promising antibacterial action against *E. coli* and *Candida*, with the ratio of a $_{90}$ZnO/$_{10}$GO compound against *E. coli* and *Staphylococcus*, and the diameter of the inhibition zone (mm) at 20 and 19 mm, respectively.

S.aureus with inhibitory zone diameters of 28 mm and 27 mm, respectively. The $_{50}$ZnO/$_{50}$GO ratio demonstrated anti-*E. coli* and anti-*Staphylococcus* action. *Staphylococcus* and *E. coli* are effectively inhibited by the other ratio, $_{70}$ZnO/$_{30}$GO, whereas *Aureus* has a diameter of the inhibition zone (mm) at 22. *Aureus* with the inhibition zone diameter (mm) at 26 and 25, respectively. Median inhibition zone (mm) against *Staphylococcus*. *Aureus*, for the ratios $_{90}$ZnO/$_{10}$GO, $_{70}$ZnO/$_{30}$GO, and $_{50}$ZnO/$_{50}$GO at 13, 14, and 14 mm, respectively.

Acknowledgment

The authors express their gratitude to the heads of the Chemistry and Physics Departments, College of Science for Women, University of Baghdad, for providing laboratory facilities for conducting scientific research and for helping them complete this work.

Conflict of Interest

The authors declare that they have no conflicts of interest.

Funding

There was no funding for the researchers.

Ethical Clearance

The authors declare that they have not used either humans or animals in any of the investigations described in this work. Also, this study was approved by the Department of Chemistry/ College of Science for Women/ University of Baghdad.

References

1. Martinelli C, Pucci C, Battaglini M, Marino A, Ciofani G. Antioxidants and nanotechnology: Promises and limits of potentially disruptive approaches in the treatment of central nervous system diseases. Adv Healthc Mater. 2020; 9(3):e1901589. https://doi.org/10.1002/adhm.201901589.
2. Choi K-H, Nam K-C, Lee S-Y, Cho G, Jung J-S, Kim H-J, Park B-J. Antioxidant potential and antibacterial efficiency of caffeic acid-functionalized ZnO nanoparticles. Nanomaterials. 2017; 7(6):148.https://doi.org/10.3390/nano7060148.
3. Phull A-R, Abbas Q, Ali A, Raza H, Kim SJ, Zia M, Haq I-U. Antioxidant, cytotoxic and antimicrobial activities of green synthesized silver nanoparticles from crude extract of Bergenia ciliata. Future J Pharm Sci. 2016; 2(1):31-36. https://doi.org/10.1016/j.fjps.2016.03.001.
4. Rehana D, Mahendiran D, Kumar RS, Rahiman A-K. In vitro antioxidant and antidiabetic activities of zinc oxide nanoparticles synthesized using different plant extracts. Bioprocess Biosyst Eng. 2017; 40(6): 943-957. https://doi.org/10.1007/s00449-017-1758-2.
5. Pelle FD, Compagnone D. Nanomaterial-based sensing and biosensing of phenolic compounds and related antioxidant capacity in food. Sensors (Basel). 2018; 18(2):462. https://doi.org/10.3390/s18020462.
6. Anjum S, Hashim M, Malik SA, Khan M, Lorenzo JM, Abbasi BH, Hano C. Recent advances in zinc oxide nanoparticles (ZnO NPs) for cancer diagnosis, target drug delivery, and treatment. Cancers (Basel). 2021; 13(18):4570. https://doi.org/10.3390/cancers13184570.
7. Zaman S. Synthesis of ZnO, CuO and their composite nanostructures for optoelectronics, sensing and catalytic applications. Linköping University (Sweden). 2012.
8. Sirelkhatim A, Mahmud S, Seeni A, Kaus NHM, Ann LC, Bakhori SKM, Hasan H, Mohamad D. Review on zinc oxide nanoparticles: Antibacterial activity and toxicity mechanism. Nanomicro Lett. 2015; 7(3):219–242. https://doi.org/10.1007/s40820-015-0040-x.
9. Yuan Y-G, Wang Y-H, Xing H-H, Gurunathan S. Quercetin-mediated synthesis of graphene oxide–silver nanoparticle nanocomposites: A suitable alternative nanotherapy for neuroblastoma. Int J Nanomedicine. 2017; 12:5819–5839. https://doi.org/10.2147/IJN.S140605.
10. Zhong L, Yun K. Graphene oxide-modified ZnO particles: Synthesis, characterization, and antibacterial properties. Int J Nanomedicine. 2015; 10(Suppl 1):79–92. https://doi.org/10.2147/IJN.S88319.
11. AlSultani MJ, Alias MFA. Impact of graphene oxide concentration and anthocyanin dye on the structural, morphological and optical properties of GO:TiO_2 thin films. Iraq J Sci. 2025; 66(6): 2336–2349. https://doi.org/10.24996/ijs.2025.66.6.12.
12. Rajeswari R, Prabu HG, Amutha DM. One-pot hydrothermal synthesis and characterization of silver nanoparticles on reduced graphene oxide for enhanced antibacterial and antioxidant properties. IOSR J Appl Chem. 2017; 10(5):64–69. https://doi.org/10.9790/5736-1005016469.

13. de Luna LAV, de Moraes ACM, Consonni SR, Pereira CD, Cadore S, Giorgio S, Alves OL. Comparative in vitro toxicity of a graphene oxide–silver nanocomposite and the pristine counterparts toward macrophages. J Nanobiotechnol. 2016; 14:12. https://doi.org/10.1186/s12951-016-0165-1.
14. Tessier F, Ray E, Cheviré F, Lemaître L, Bonnier F, Bazer-Bachi D, Lecocq V. Transesterification of vegetable oils by AlPOxNy heterogeneous catalysts. Appl Catal B Env. 2016; 185:253-264. https://doi.org/10.1016/j.apcatb.2015.12.024.
15. Valenzuela L, Iglesias-Juez A, Bachiller-Baeza B, Faraldos M, Bahamonde A, Rosal R. Biocide mechanism of antimicrobial surfaces based on zinc oxide–reduced graphene oxide photocatalytic coatings. J Mater Chem B. 2020; 8(36):8294–8304. https://doi.org/10.1039/D0TB01262A.
16. Sanchez JA, Materon L, Parsons JG, Alcoutlabi M. Synthesis, characterization, and antibacterial activity of graphene oxide/zinc hydroxide nanocomposites. Appl Sci. 2024; 14(14):6274. https://doi.org/10.3390/app14146274.
17. Ruan S, Zhao Y, Chen R, Ma J, Guan Y, Ma J, Ren L. Effect of zinc oxide/graphene oxide nanocomposites on the cytotoxicity, antibacterial and mechanical properties of polymethyl methacrylate. BMC Oral Health. 2024; 24(1):1013. https://doi.org/10.1186/s12903-024-04754-0.
18. Tareq S, Mousa SA, Muhammed EA. Synthesis catalyst of loading nano platinum on graphene nanosheets and photodegradation of bromophenol blue in ultra-violet light. Baghdad Sci J. 2024; 21(11): 3356-3367.https://doi.org/10.21123/bsj.2024.9866.
19. Hao Y, Wang Y, Zhang L, Liu F, Jin Y, Long J, Chen S, Duan G, Yang H. Advances in antibacterial activity of zinc oxide nanoparticles against Staphylococcus aureus (Review). Biomed Rep. 2024; 21(5):161. https://doi.org/10.3892/br.2024.1849.
20. Byun J. Emerging frontiers of graphene in biomedicine. J Microbiol Biotechnol. 2015; 25(2):145–151. https://doi.org/10.4014/jmb.1412.12045.
21. Parashar M, Shukla VK, Singh R. Metal oxides nanoparticles via sol–gel method: A review on synthesis, characterization and applications. J Mater Sci: Mater Electron. 2020; 31:3729–3749. https://doi.org/10.1007/s10854-020-02994-8.
22. Abbas SR, Oleiwi HF. ZnO nanorod arrays for gas sensor application growing via hydrothermal technique: Effect of metal oxide decoration. J Opt. 2024; 1–11. https://doi.org/10.1007/s12596-024-02341-8.
23. Mahafel N, Vaezi Z, Barzegar M, Hekmat A, Naderi-Manesh H. Synergistic antibacterial effect of the pistachio green hull extract-loaded porphysome decorated with 4-nitroimidazole against bacteria. J Liposome Res. 2024; 34(3):475–488. https://doi.org/10.1080/08982104.2024.2304755.
24. Ali A, Chiang YW, Santos RM. X-ray diffraction techniques for mineral characterization: A review for engineers of the fundamentals, applications, and research directions. Minerals. 2022; 12(2):205. https://doi.org/10.3390/min12020205.
25. Mustapha S, Ndamitso MM, Abdulkareem AS, Oladejo JT, Shuaib DY, Mohammed AK, Sumaila A. Comparative study of crystallite size using Williamson-Hall and Debye-Scherrer plots for ZnO nanoparticles. Adv Nat Sci Nanotechnol. 2019; 10(4):045013. https://doi.org/10.1088/2043-6254/ab52f7.
26. Shadmehri AA, Namvar F, Miri H, Yaghmaei P, Moghaddam MN. Assessment of antioxidant and antibacterial activities of zinc oxide nanoparticles, graphene and graphene decorated by zinc oxide nanoparticles. Int J Nano Dimens. 2019; 10:350–358.
27. Al-Mashhadani TA, Kadhum FM, Jawad AA, Ajeel K, Mohsen AH. Investigating the antibacterial activity of zinc oxide nanoparticles against Staphylococcus aureus isolates. J Biosci Appl Res. 2025; 11(1):270–280. https://doi.org/10.21608/jbaar.2025.419993.
28. Gujrati A, Khanal SR, Pastewka L, Jacobs TDB. Combining TEM, AFM, and profilometry for quantitative topography characterization across all scales. ACS Appl Mater Interfaces. 2018; 10(34): 29169-29178. https://doi.org/10.1021/acsami.8b09899.
29. Bhatt S, Punetha VD, Pathak R, Punetha M. Graphene in nanomedicine: A review on nano-bio factors and antibacterial activity. Colloids Surf B Biointerfaces. 2023; 226:113323. https://doi.org/10.1016/j.colsurfb.2023.113323.
30. Manna, A.C. Synthesis, characterization, and antimicrobial activity of zinc oxide nanoparticles. In: Cioffi, N., Rai, M. (eds) Nano-Antimicrobials. Springer, Berlin, Heidelberg. 2012. https://doi.org/10.1007/978-3-642-24428-5_5.